Frontiers in Bioscience Landmark

Front. Biosci. (Landmark Ed) **2026**; 31(9): 54255
https://doi.org/10.31083/FBL54255

Original Research

Multi-Omics Analyses Reveal Expression Remodeling of Key Glycolytic-Lactate Metabolic Nodes in the Pituitary of High-Altitude Sheep

Fengyu Mao[1], Xia Liu[1,*], Xiaohua Du[2], Haifang Wang[1]

[1]College of Life Science and Technology, Gansu Agricultural University, 730070 Lanzhou, Gansu, China
[2]College of Veterinary Medicine, Gansu Agricultural University, 730070 Lanzhou, Gansu, China
*Correspondence: liux@gsau.edu.cn (Xia Liu)

Academic Editor: Gianluca Paventi
Submitted: 26 May 2026 Revised: 16 July 2026 Accepted: 24 July 2026 Published: 7 September 2026

Abstract

Background: Most studies of high-altitude adaptation in animals have focused on the heart, lung, blood, and skeletal muscle, whereas systematic evidence regarding metabolism-related expression changes in the pituitary remains limited. The pituitary is an energy-demanding neuroendocrine organ characterized by active glucose utilization and lactate production. However, multi-omics changes associated with glycolysis–lactate metabolism in the pituitary of high-altitude sheep remain undefined. **Methods:** Pituitary tissues from adult female sheep living at high altitude were compared with those from adult female sheep living at low altitude (n = 3 per group). Transcriptomic differences were profiled by RNA sequencing, and proteomic differences were characterized by data-independent acquisition (DIA) mass spectrometry (MS). Gene Ontology and Kyoto Encyclopedia of Genes and Genomes enrichment analyses, gene set enrichment analysis, and integrated transcriptomic–proteomic analyses were used to identify representative candidates, which were further validated by reverse transcription quantitative polymerase chain reaction and western blotting. **Results:** RNA sequencing identified 1222 differentially expressed genes, including 690 upregulated and 532 downregulated genes, whereas DIA-MS identified 2046 differentially expressed proteins, including 1096 upregulated and 950 downregulated proteins. Functional analyses indicated enrichment of glycolysis, lactate metabolism, pyruvate metabolism, the HIF-1 signaling pathway, and oxidative phosphorylation. Gene set enrichment analysis showed significant positive enrichment of oxidative phosphorylation in the high-altitude group, whereas glycolysis/gluconeogenesis showed a positive trend without meeting the false discovery rate threshold. Integrated transcriptomic–proteomic analysis identified hexokinase 2 (HK2), enolase 2 (ENO2), and lactate dehydrogenase A (LDHA) as concordantly upregulated at both the transcript and protein levels (q-value < 0.05). Reverse transcription quantitative PCR (RT-qPCR) showed significant upregulation of *HK2*, *ENO2*, and *LDHA* (all $p < 0.001$), while western blotting confirmed increased protein expression, with HK2 reaching $p < 0.001$ and ENO2 and LDHA reaching $p < 0.01$. **Conclusions:** HK2, ENO2, and LDHA are stably upregulated in the pituitary of high-altitude sheep, indicating remodeling of key expression nodes associated with glycolysis–lactate metabolism. These findings provide multi-omics evidence for high-altitude-associated remodeling of selected metabolic expression nodes in the sheep pituitary.

Keywords: high-altitude sheep; pituitary; glycolysis; lactate metabolism; RNA-seq; DIA-MS

1. Introduction

Animals living at high altitude are chronically exposed to a hypobaric hypoxic environment, and their adaptation involves multilevel adjustments in morphology, cardiorespiratory function, and energy metabolism [1,2]. Activation of hypoxia-responsive signaling pathways is an important molecular basis of this process. Under hypoxic conditions, regulatory factors such as hypoxia-inducible factor 1 (HIF-1) are activated and induce a series of transcriptional changes associated with oxygen homeostasis and energy metabolism [3,4]. In this context, glycolysis and lactate metabolism are commonly regarded as important components of metabolic adjustment under limited oxygen availability, although their expression patterns are not fully consistent across tissues and species [5,6,7].

The pituitary is a key neuroendocrine organ that maintains endocrine homeostasis, and the synthesis, processing, and secretion of pituitary hormones depend on a stable energy supply. Early *in vivo* metabolic studies showed that a substantial proportion of glucose taken up by the pituitary can be converted into lactate, suggesting active glucose utilization and lactate production in this tissue [8]. Subsequent hypoxia-related studies further showed that the expression of transcription factors, hormones, and their receptors in the adult rat pituitary can change after hypoxic exposure, indicating that pituitary endocrine function is responsive to altered oxygen availability [9]. However, under long-term hypoxic conditions, integrated transcriptomic and proteomic evidence for coordinated changes in glycolysis–lactate metabolism-related molecules in the sheep pituitary is still lacking.

Recent multi-tissue omics studies in high-altitude animals have shown that adaptation to hypoxia does not occur in a single organ, but involves transcriptional reg-

ulation and metabolism-related remodeling across multiple tissue systems [2]. Existing studies in high-altitude sheep have mainly focused on the heart, lung, blood, and multi-tissue comparisons, whereas systematic evidence for metabolism-related molecular expression in the pituitary remains limited. To address this gap, pituitary tissues from high-altitude sheep were compared with those from low-altitude sheep by integrated transcriptomic and proteomic analysis. The present study focused on molecules associated with the glycolysis–lactate metabolism axis, and key candidates were further validated by reverse transcription quantitative PCR (RT-qPCR) and western blotting. This framework was designed to characterize glycolysis–lactate metabolism-related expression differences in the pituitary of naturally reared high-altitude and low-altitude sheep. The study therefore provides molecular evidence for high-altitude-associated metabolic remodeling in neuroendocrine tissue.

2. Materials and Methods

2.1 Animals and Pituitary Sample Collection

Healthy adult female sheep approximately 1 year of age were used in this study. The high-altitude group (HA) consisted of Oula sheep native to the Qilian pastoral area of Qinghai, where the average sampling altitude was approximately 3400 m. The low-altitude (LA) group consisted of Hu sheep from Lanzhou, Gansu, where the average sampling altitude was approximately 1200 m. Three sheep were included in each group, for a total of six animals, and each animal served as an independent biological replicate.

Adult non-pregnant ewes of a similar age were included to reduce biological variation associated with sex, age, and reproductive status. All animals were sampled during the same season at their respective rearing sites. The pituitary samples were obtained through locally routine breeding and production procedures. Pituitary tissues were rapidly frozen in liquid nitrogen after collection and stored at −80 °C for subsequent RNA sequencing (RNA-seq), Data-Independent Acquisition Mass Spectrometry (DIA-MS), RT-qPCR, and Western blot analyses. The animal experimental protocol was approved by the Animal Ethics Committee of Gansu Agricultural University (approval No. GSAU-Eth-LST-2023-004).

2.2 RNA Sequencing and Transcriptomic Analysis

Total RNA was extracted from pituitary tissues using TransZol reagent (TransGen Biotech Co., Ltd., Beijing, China; Cat. No. ET101). For each sample, part of the RNA was reverse-transcribed for RT-qPCR validation, whereas the remainder was used for transcriptome sequencing. RNA integrity and quality were assessed using an Agilent 2100 Bioanalyzer, and qualified samples were used for library construction. Libraries were sequenced on an Illumina platform with a paired-end 150 bp strategy.

Raw sequencing data were processed with fastp [10] to remove adapter sequences and low-quality reads and to obtain clean reads. Ribosomal RNA sequences were removed after alignment with Bowtie2 [11]. Filtered reads were then aligned to the sheep reference genome (GCF_016772045.2) using HISAT2 [12]. Gene expression levels were quantified with RSEM [13] and expressed as fragments per kilobase of transcript per million mapped reads. Differentially expressed genes were identified from the gene count matrix using DESeq2 [14]. Genes with a fold change ≥ 2 or ≤ 0.5 and a q value < 0.05 were considered differentially expressed. Principal component analysis (PCA) was used to evaluate global expression patterns, within-group reproducibility, and between-group separation.

2.3 DIA-MS Proteomic Analysis

Pituitary tissues were homogenized in radioimmunoprecipitation assay (RIPA) lysis buffer supplemented with PMSF (Solarbio Science & Technology Co., Ltd., Beijing, China; Cat. No. R0010) to extract total protein. For each sample, one portion of the protein extract was used for western blot validation and the remainder was used for DIA-MS analysis. After enzymatic digestion, peptides were separated using an UltiMate 3000 UHPLC system (Thermo Fisher Scientific, Waltham, MA, USA) and analyzed on a Bruker timsTOF Pro2 (Bruker Daltonics GmbH & Co. KG, Bremen, Germany) mass spectrometer in data-independent acquisition mode [15]. iRT standard peptides [16] were added to each sample for retention-time calibration to improve cross-sample quantitative comparability.

Proteomic raw data were first subjected to quality control assessment using QuiC software (Biognosys AG, Schlieren, Zurich, Switzerland) [17] to confirm instrument stability and sample reproducibility. DIA data were then processed with Spectronaut for spectral library matching, protein identification, and quantitative analysis. Identifications at both precursor and protein levels were accepted at a false discovery rate of 1.0%. Signal intensities were normalized using the local normalization method, and relative protein abundances were calculated based on peptides and precursors that satisfied false discovery rate (FDR) control criteria. Differential expression analysis was performed on the normalized protein abundance matrix. Proteins with a fold change ≥ 1.2 or ≤ 0.83 and a q value < 0.05 were considered differentially expressed proteins. PCA was used to visualize overall protein expression patterns and between-group separation.

2.4 Functional Enrichment, GSEA, and Selection of Glycolysis–Lactate Metabolism Candidates

Gene Ontology (GO) annotation [18] and Kyoto Encyclopedia of Genes and Genomes (KEGG) pathway enrichment analysis [19] were performed separately for differentially expressed genes (DEGs) and differentially expressed proteins (DEPs) to identify the major biological processes

Table 1. Primer sequences and amplification parameters.

Gene	Forward Primer 5′–3′	Reverse Primer 5′–3′	Annealing temperature (°C)	Product length (bp)
HK2	GGGGTTCAAGTCCAGTGGTG	AGAGCCCATGTCGATCTCCT	60	337
ENO2	ACTCAGACCTCATCCTGCCTGT	GTCCTTGCCATACTTGTCCTTGAT	60	191
LDHA	GTCTGAATTTGGTCCAGCGTAAC	TATCTTCCAAGCCACATAGGTCA	60	134
β-actin	ATATTGCTGCGCTCGTGGTT	GTTGGTGACAATGCCGTGCT	60	224

and pathways represented by the differential molecules between the high-altitude (HA) and LA groups. Enrichment was considered significant at q value < 0.05.

To assess overall pathway-level expression trends, gene set enrichment analysis (GSEA) [20] was further performed based on ranked transcriptome-wide gene expression. Particular attention was paid to gene sets associated with glycolysis/gluconeogenesis, the HIF-1 signaling pathway, pyruvate metabolism, and oxidative phosphorylation. GSEA results were reported as enrichment score (ES), normalized enrichment score (NES), p value, and FDR q value.

Candidate molecules were selected according to statistical significance, pathway relevance, and expression direction. Molecules showing concordant changes at the transcript and protein levels were prioritized for targeted validation because they provided consistent evidence across both omics datasets.

2.5 Integrated Transcriptomic-Proteomic Analysis

All molecules matched between the RNA-seq and DIA-MS datasets were classified as co-upregulated, co-downregulated, transcript-up/protein-down, or transcript-down/protein-up. Concordant molecules were prioritized for experimental validation, while discordant categories were retained in the integrated analysis.

2.6 RT-qPCR and Western Blot Validation

Based on the integrated transcriptomic-proteomic analysis, hexokinase 2 (HK2), enolase 2 (ENO2), and lactate dehydrogenase A (LDHA) were selected as representative candidate molecules for RT-qPCR system (Thermo Fisher Scientific, Guangzhou, Guangdong, China) and Western blot validation. The mRNA sequences of *HK2*, *ENO2*, *LDHA*, and *β-actin* were obtained from the National Center for Biotechnology Information (NCBI) database under accession numbers XM_015094476.3, XM_012175500.5, XM_042238239.1, and NM_001009784.3, respectively. Specific primers were designed using Primer Premier 5.0 (PREMIER Biosoft International, Palo Alto, CA, USA). Primer sequences are shown in Table 1.

Total RNA was reverse-transcribed into cDNA using a first-strand cDNA synthesis kit, and RT-qPCR was performed using a universal dye-based quantitative PCR premix. The amplification program consisted of 95 °C for 30 s, followed by 40 cycles of 95 °C for 5 s and 60 °C for 30 s. Product specificity was confirmed by melt-curve analysis and agarose gel electrophoresis. *β-actin* was used as the internal reference gene, and relative expression levels of HK2, ENO2, and LDHA were calculated using the $2^{-\Delta\Delta Ct}$ method.

For western blot validation, total protein was extracted from pituitary tissues, separated by sodium dodecyl sulfate–polyacrylamide gel electrophoresis (SDS-PAGE), and transferred onto polyvinylidene difluoride (PVDF) membranes. After blocking with 5% skim milk, membranes were incubated with primary antibodies against HK2, ENO2, LDHA, and β-actin, followed by incubation with horseradish peroxidase-conjugated secondary antibody. Signals were visualized using an enhanced chemiluminescence (ECL) reagent (Oriscience Biotechnology Co., Ltd., Chengdu, Sichuan, China; Cat. No. PD203-120 mL) and captured with a chemiluminescence imaging system (VILBER Bio Imaging, Collégien, France). Band intensities were quantified with ImageJ version 1.47 (U.S. National Institutes of Health, Bethesda, MD, USA) [21] and normalized to β-actin. Antibody information is listed in Table 2.

2.7 Statistical Analysis

Except for omics-based differential-expression analyses, RT-qPCR and Western blot validation data are presented as mean ± standard deviation. Comparisons between the HA and LA groups were performed using a two-sided Student's t test, with n = 3 per group. A p value < 0.05 was considered statistically significant. GraphPad Prism 8.0 1 (GraphPad Software, San Diego, CA, USA) was used for statistical analysis and figure generation. Statistical significance in the figures is indicated as follows: * $p < 0.05$, ** $p < 0.01$, and *** $p < 0.001$.

3. Results

3.1 Distinct Transcriptomic Profiles in Pituitaries From High-Altitude Sheep

A total of six pituitary transcriptome libraries were constructed in this study. Sequencing generated approximately 3.7×10^7 to 4.4×10^7 paired-end 150 bp reads per sample. After quality filtering, approximately 2.43×10^8 clean reads were retained. Guanine-Cytosine (GC) content ranged from 49.1% to 49.6%, Q30 values were all above 94.6%, total alignment rates exceeded 96.5%, and unique alignment rates were approximately 92%, indicating that the RNA-seq data were of sufficient quality for subsequent expression quantification and differential analysis.

Table 2. Antibodies used for Western blotting.

Antibody	Host species	Clone/Catalog No.	Manufacturer	Dilution
HK2	Rabbit monoclonal	TB4376	Abmart Biotech Co., Ltd.	1:1000
ENO2	Rabbit monoclonal	T55656	Abmart Biotech Co., Ltd.	1:1000
LDHA	Rabbit monoclonal	T55348	Abmart Biotech Co., Ltd.	1:1000
β-actin	Rabbit polyclonal	bs-0061R	Bioss Biotechnology Co., Ltd.	1:5000
Goat Anti-Rabbit IgG HRP	Goat anti-rabbit	M21002	Abmart Biotech Co., Ltd.	1:3000

HK2, hexokinase 2; ENO2, enolase 2; LDHA, lactate dehydrogenase A; HRP, horseradish peroxidase.

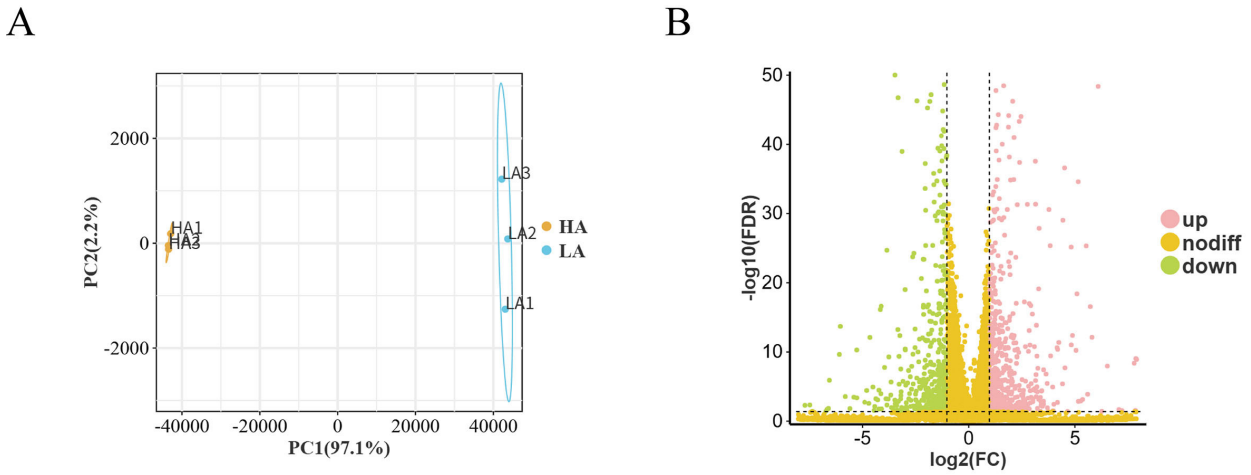

Fig. 1. Distinct transcriptomic profiles in pituitaries from high-altitude sheep. (A) PCA of pituitary samples from the HA and LA groups. (B) Volcano plot of DEGs in the HA group relative to the LA group. Pink indicates genes upregulated in the HA group, green indicates genes downregulated in the HA group, and yellow indicates genes without significant differential expression. PCA, principal component analysis; HA, high-altitude group; LA, low-altitude; FDR, false discovery rate; DEGs, differentially expressed genes.

PCA showed clear separation between the HA and LA groups, with good within-group clustering, suggesting distinct global transcriptomic profiles in the pituitary between the two groups (Fig. 1A). Using a fold change threshold of ≥ 2 or ≤ 0.5 and q value < 0.05, 1222 DEGs were identified, including 690 genes upregulated and 532 genes downregulated in the HA group. The volcano plot further illustrated the fold changes and statistical significance of the DEGs (Fig. 1B). These results indicate that the pituitary of HA sheep displays pronounced transcriptomic differences relative to that of LA sheep.

3.2 Functional Enrichment of Differentially Expressed Genes

To define the major biological processes represented by the DEGs, GO and KEGG enrichment analyses were performed for the 1222 DEGs. GO biological process enrichment showed that the DEGs were associated with the glycolytic process, transmembrane glucose transport, pyruvate metabolic process, and lactate/monocarboxylate transport, all of which are closely related to the glycolysis–lactate metabolism axis. Terms related to response to hypoxia, ATP metabolic process, and oxidative phosphorylation were also enriched, indicating alterations related to both energy metabolism and oxygen availability.

KEGG pathway analysis further showed that glycolysis–lactate metabolism-related DEGs were mainly enriched in the HIF-1 signaling pathway, glycolysis/gluconeogenesis, carbon metabolism, oxidative phosphorylation, and pyruvate metabolism (Fig. 2). Over-representation analysis identified the HIF-1 signaling pathway and glycolysis/gluconeogenesis among pathways containing a relatively high proportion of differential molecules. However, over-representation of pathway-annotated molecules does not demonstrate activation of HIF-1 signaling or coordinated activation of the entire glycolytic pathway. Consistent with this distinction, transcriptome-wide GSEA did not identify significant enrichment of the HIF-1 signaling gene set.

To further assess pathway-level expression trends, KEGG-GSEA was performed using transcriptome-wide ranked gene expression for the four prespecified metabolism-related gene sets. Oxidative phosphorylation showed significant positive enrichment in the HA group (NES = 1.60, FDR q value = 0.019). Glycolysis/gluconeogenesis showed a positive enrichment trend but did not reach FDR significance (NES = 1.35, FDR q value = 0.151), whereas the HIF-1 signaling and pyruvate metabolism gene sets were not significantly enriched. These non-significant results were retained in the interpre-

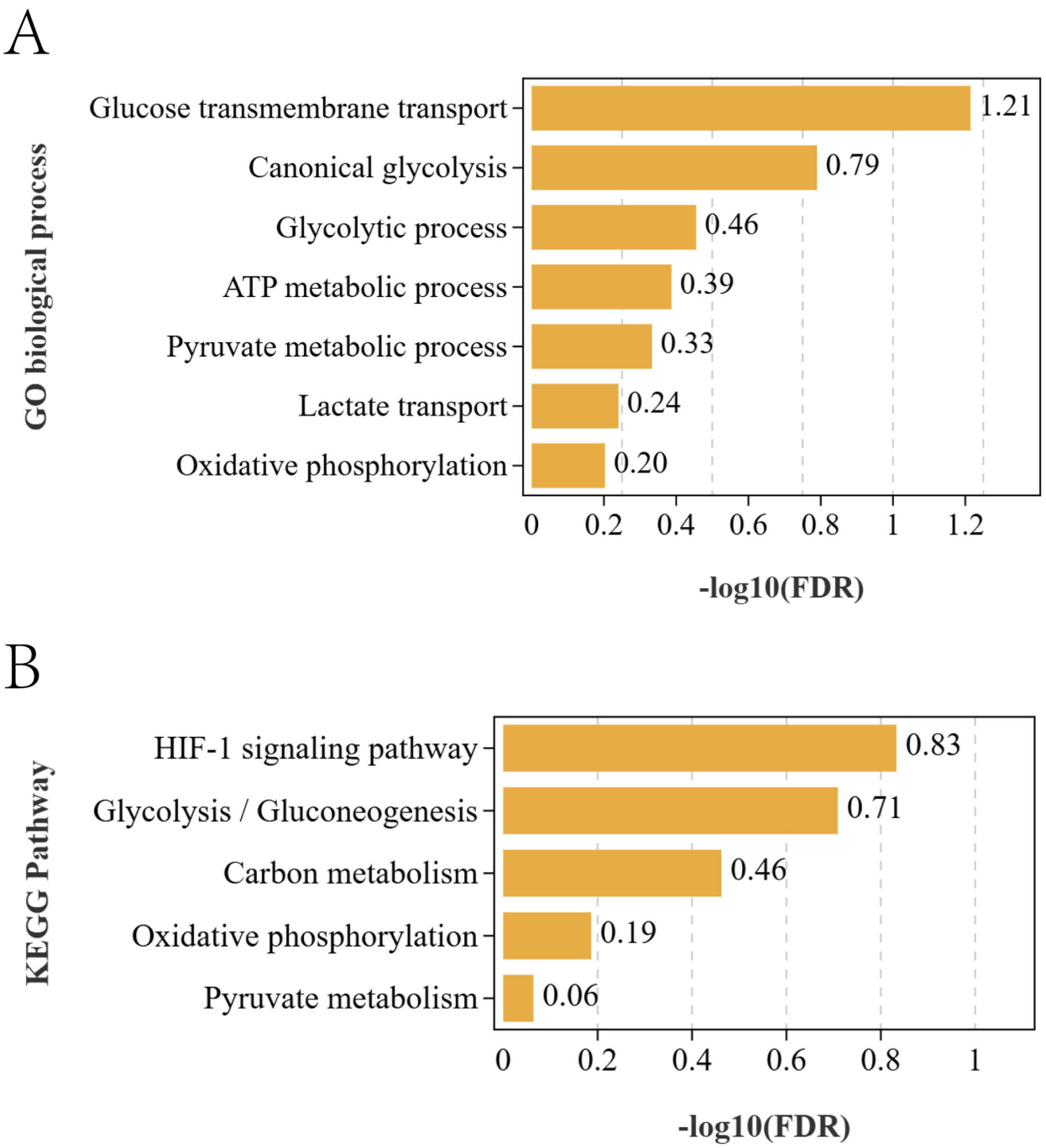

Fig. 2. Functional enrichment of glycolysis–lactate metabolism-related DEGs in the sheep pituitary. (A) GO enrichment analysis of glycolysis–lactate metabolism-related DEGs. (B) KEGG pathway enrichment analysis of glycolysis–lactate metabolism-related DEGs. Larger x-axis values indicate stronger enrichment relevance. GO, Gene Ontology; KEGG, Kyoto Encyclopedia of Genes and Genomes.

tation to avoid equating over-representation of differential genes with coordinated pathway-wide activation (Fig. 3).

3.3 Differential Proteomic Profiles and Functional Enrichment

Proteomic analysis showed clear separation of the HA and LA groups in PCA space, indicating global differences in pituitary protein expression between the two groups (Fig. 4A). Using a fold change threshold of ≥1.2 or ≤0.83 and q value < 0.05, 2046 DEPs were identified, including 1096 upregulated and 950 downregulated proteins in the HA group. The volcano plot further illustrated the distribution of fold changes and statistical significance for the DEPs (Fig. 4B). These results indicate that significant between-group differences were also present at the proteomic level.

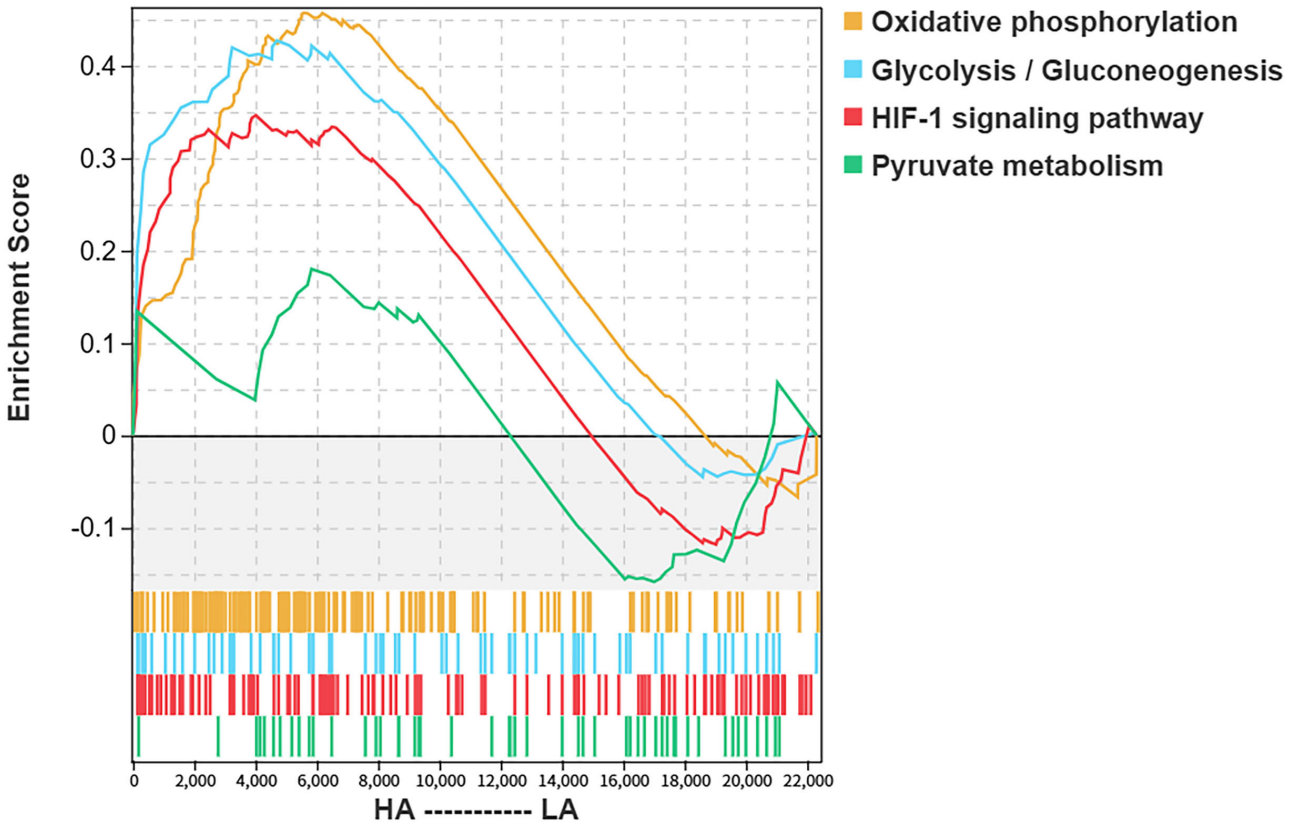

Fig. 3. GSEA of energy metabolism-related KEGG pathways in the sheep pituitary. GSEA was performed on oxidative phosphorylation, glycolysis/gluconeogenesis, the HIF-1 signaling pathway, and pyruvate metabolism based on transcriptome-wide ranked gene expression. GSEA, gene set enrichment analysis; HIF-1, hypoxia-inducible factor 1.

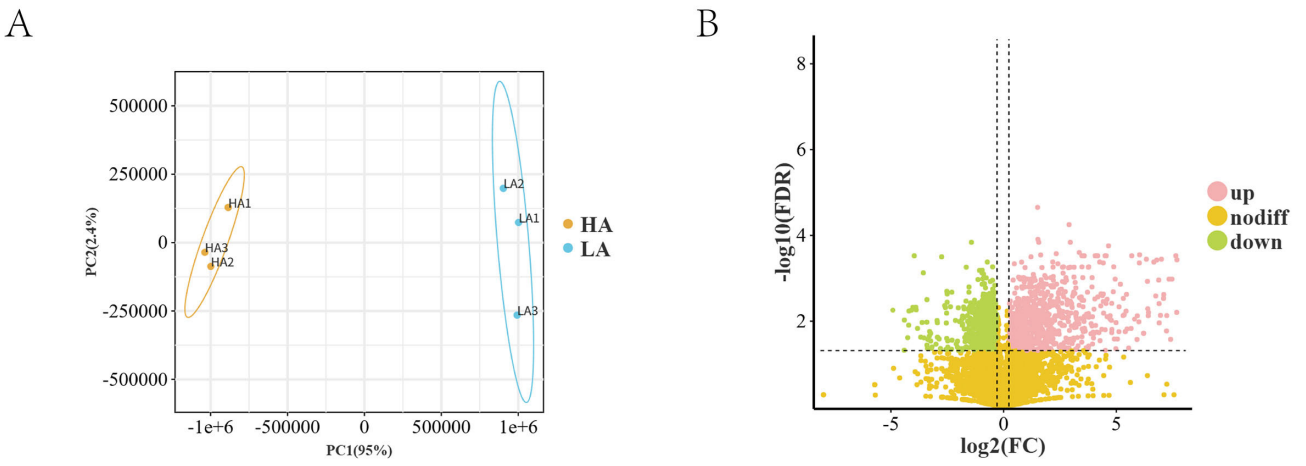

Fig. 4. Differential proteomic profiles in pituitaries from high-altitude sheep. (A) PCA of pituitary proteomes from the HA and LA groups. (B) Volcano plot of DEPs in the HA group relative to the LA group. Pink indicates proteins upregulated in the HA group, green indicates proteins downregulated in the HA group, and yellow indicates proteins without significant differential expression. DEPs, differentially expressed proteins.

GO and KEGG enrichment analyses of the DEPs further showed that the affected proteins were associated with oxidation-reduction processes, canonical glycolysis, lactate metabolic process, pyruvate metabolic process, and the glycolytic process (Fig. 5A). KEGG analysis indicated enrichment in carbon metabolism, glycolysis/gluconeogenesis,

Table 3. Multi-omics consistency of representative candidate molecules related to glycolysis–lactate metabolism.

Molecule	RNA-seq trend	RNA-seq log2 FC	RNA-seq q value	DIA-MS trend	DIA-MS log2 FC	DIA-MS q value
HK2	↑	2.244508	0.000011	↑	2.152741	0.048835
ENO2	↑	1.306755	1.6215×10^{-16}	↑	1.740137	0.015719
LDHA	↑	1.909935	8.4753×10^{-45}	↑	4.167096	0.000309

Note: ↑ indicates upregulation in the HA group relative to the LA group. $\log_2$ FC denotes the expression change in the HA group relative to the LA group. q value indicates the significance level after multiple-testing correction.

the HIF-1 signaling pathway, and pyruvate metabolism (Fig. 5B). These results provided the basis for subsequent selection of representative molecules associated with the glycolysis–lactate metabolism axis by integrating directional protein changes with transcriptomic-proteomic concordance.

3.4 Multi-Omics Concordance of Representative Glycolysis–Lactate Metabolism Nodes

Integrated transcriptomic-proteomic analysis showed that HK2, ENO2, and LDHA were all located in the co-upregulated quadrant (Fig. 6). These molecules were selected for validation because they showed significant concordant changes in both datasets and represented distinct steps within glycolysis–lactate metabolism. Detailed expression changes and statistical results for these three molecules in the RNA-seq and DIA-MS datasets are summarized in Table 3.

3.5 Experimental Validation of HK2, ENO2, and LDHA

To validate the multi-omics results, HK2, ENO2, and LDHA were further examined by RT-qPCR and western blotting. RT-qPCR showed that the mRNA expression levels of *HK2*, *ENO2*, and *LDHA* differed between the LA and HA groups, with all three being significantly higher in the HA group. Among them, *HK2*, *ENO2*, and *LDHA* all showed highly significant differences ($p < 0.001$). These results were consistent with the transcriptomic findings (Fig. 7).

Western blot analysis further showed that the protein expression levels of HK2, ENO2, and LDHA were all higher in the HA group than in the LA group. HK2 reached $p < 0.001$, whereas ENO2 and LDHA reached $p < 0.01$. These validation results were consistent with the proteomic data (Fig. 8).

4. Discussion

In the present study, integrated RNA-seq and DIA-MS analyses showed that HK2, ENO2, and LDHA were consistently upregulated in the pituitary samples of the adult female HA sheep examined in this study. HK2, ENO2, and LDHA occupy the glycolytic entry step, the later glycolytic phase, and the pyruvate-to-lactate conversion step, respectively. Their concurrent upregulation therefore indicates that expression changes related to glycolysis–lactate metabolism involve multiple contiguous metabolic nodes in the pituitary of high-altitude sheep. Over-representation analysis linked a subset of differential molecules to the HIF-1 signaling pathway. Transcriptome-wide GSEA did not show significant enrichment of this gene set. Since HIF-1α protein stabilization, nuclear localization, and transcriptional activity were not examined, the present data do not establish HIF-1 activation or direct regulation of HK2, ENO2, and LDHA. Further verification will require controlled hypoxia models and targeted analysis of HIF-1α activity [22,23]. Discordant transcript–protein patterns were also observed and may reflect differences in translation efficiency, protein stability, or degradation. Further experiments are required to determine the mechanisms underlying these discrepancies.

Within these contiguous metabolic nodes, upregulation of LDHA requires particularly cautious interpretation in light of the multiple functions of lactate metabolism [24]. Recent studies have shown that lactate is not merely the end product of glycolysis. It can also serve as an oxidative substrate and as an important mediator of inter-tissue and intercellular metabolite transport and signaling [25,26,27]. Accordingly, the concurrent upregulation of LDHA with HK2 and ENO2 in this study is better interpreted as an adjustment of expression nodes related to the terminal stage of glycolysis and pyruvate-to-lactate conversion, rather than direct evidence of increased lactate content or enhanced lactate metabolic flux. Considering the known characteristics of active glucose utilization and lactate production in the pituitary [8], these results suggest that glycolysis–lactate metabolism-related nodes may participate in local energy-metabolic adaptation of the pituitary under long-term high-altitude conditions.

The pathway-level results do not support a uniform shift from oxidative metabolism to glycolysis. KEGG-GSEA showed significant positive enrichment of oxidative phosphorylation in the HA group, whereas glycolysis/gluconeogenesis showed only a positive trend that did not meet the FDR threshold. The HIF-1 signaling and pyruvate metabolism gene sets were also not significantly enriched by GSEA. These findings indicate that the upregulation of HK2, ENO2, and LDHA should be interpreted as remodeling of selected glycolysis–lactate-related expression

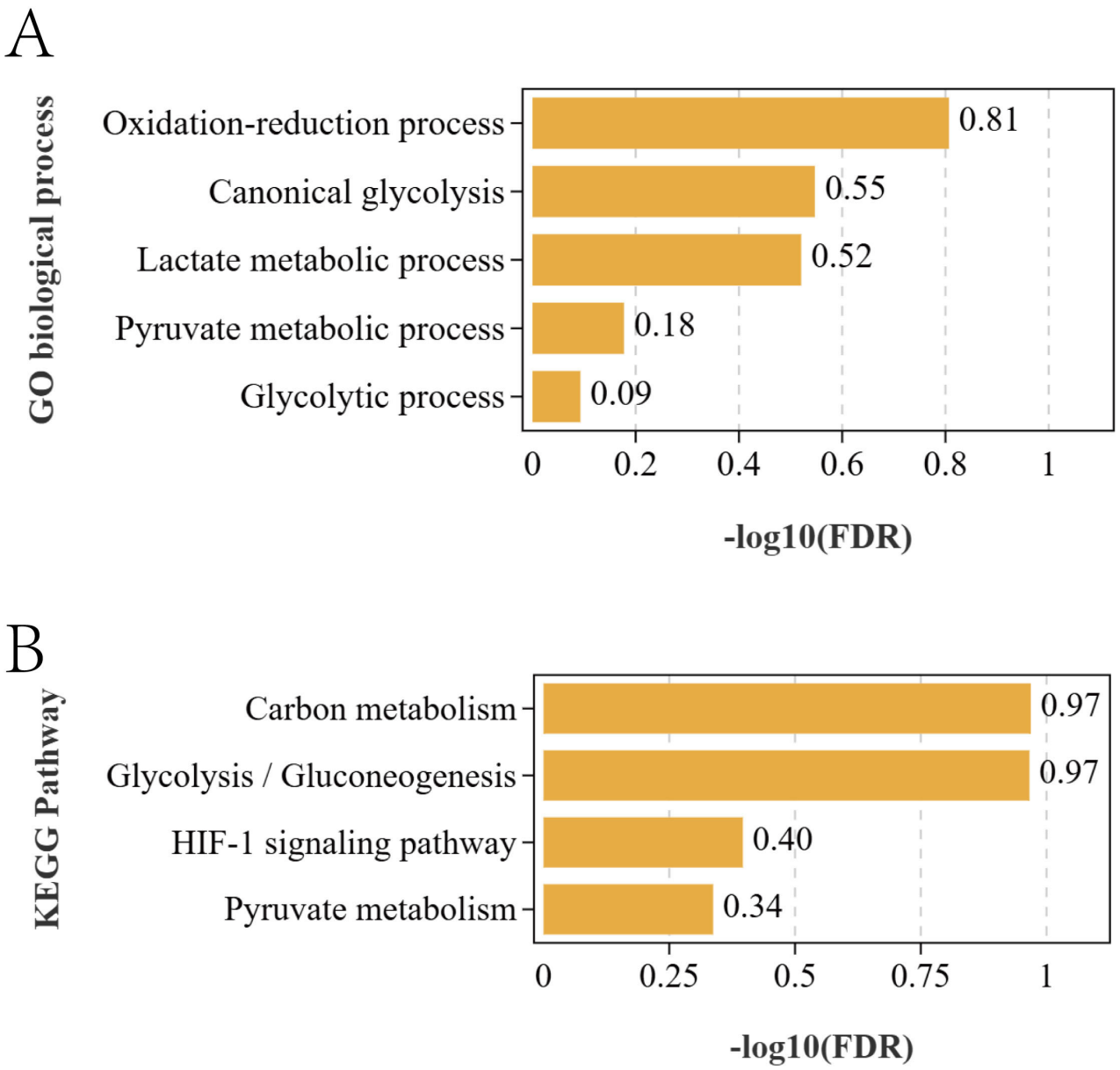

Fig. 5. Functional enrichment of glycolysis–lactate metabolism-related DEPs in the sheep pituitary. (A) GO enrichment analysis of glycolysis–lactate metabolism-related DEPs. (B) KEGG pathway enrichment analysis of glycolysis–lactate metabolism-related DEPs. Larger x-axis values indicate stronger enrichment relevance.

nodes rather than coordinated activation of the entire glycolytic pathway. The concurrent positive enrichment of oxidative phosphorylation further suggests that selected glycolytic and lactate-related changes may coexist with maintenance or compensatory adjustment of mitochondrial energy metabolism. Because lactate can also serve as an oxidative substrate and contribute carbon to the tricarboxylic acid cycle, glycolysis–lactate metabolism and oxidative phosphorylation should not necessarily be regarded as mutually exclusive or strictly antagonistic processes [28,29]. Nevertheless, expression enrichment cannot determine actual pathway flux or establish direct functional interactions between these metabolic systems.

The pituitary is a key neuroendocrine organ required for endocrine homeostasis, and its hormone synthesis, processing, and secretion all depend on a sustained energy supply. Previous studies of high-altitude adaptation have mainly focused on respiratory and circulatory functions, oxygen transport, and peripheral metabolic tissues, whereas comparatively less attention has been paid to metabolism-related expression features in neuroendocrine organs such as the pituitary [30,31,32]. The present results suggest that the pituitary may undergo metabolism-related expression adjustment in response to local energy demands during long-term residence at high altitude. Future studies combining metabolite measurements, enzyme activity assays,

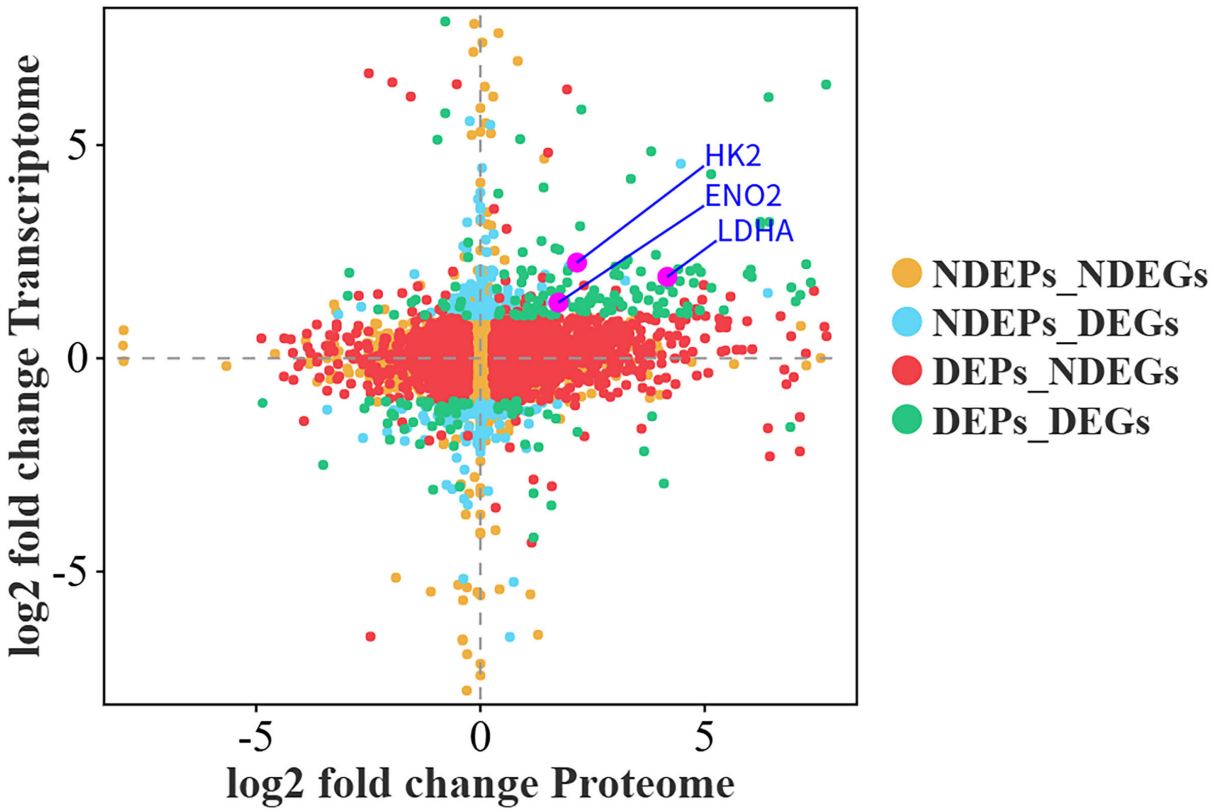

Fig. 6. Integrated transcriptomic-proteomic analysis of representative candidate molecules related to glycolysis–lactate metabolism. The four-quadrant plot shows the distribution of matched molecules according to transcriptomic and proteomic log2 FC values. HK2, ENO2, and LDHA are all located in the co-upregulated quadrant.

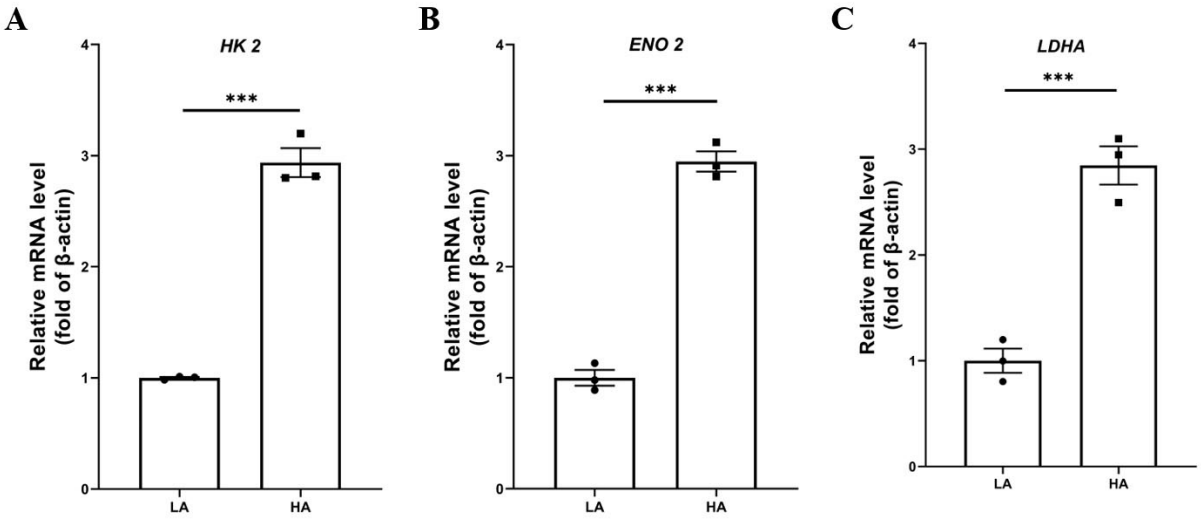

Fig. 7. RT-qPCR validation of *HK2*, *ENO2*, and *LDHA* expression in sheep pituitaries. (A) Relative mRNA expression of *HK2* in the LA and HA groups. (B) Relative mRNA expression of ENO2 in the LA and HA groups. (C) Relative mRNA expression of LDHA in the LA and HA groups. β-actin was used as the internal reference gene. *** $p < 0.001$. RT-qPCR, reverse transcription quantitative PCR.

and functional experiments will be needed to clarify the relationship between these expression changes and pituitary endocrine regulation.

Several aspects of the study should be considered when interpreting the findings. The analysis was conducted in adult non-pregnant ewes, with three animals included in

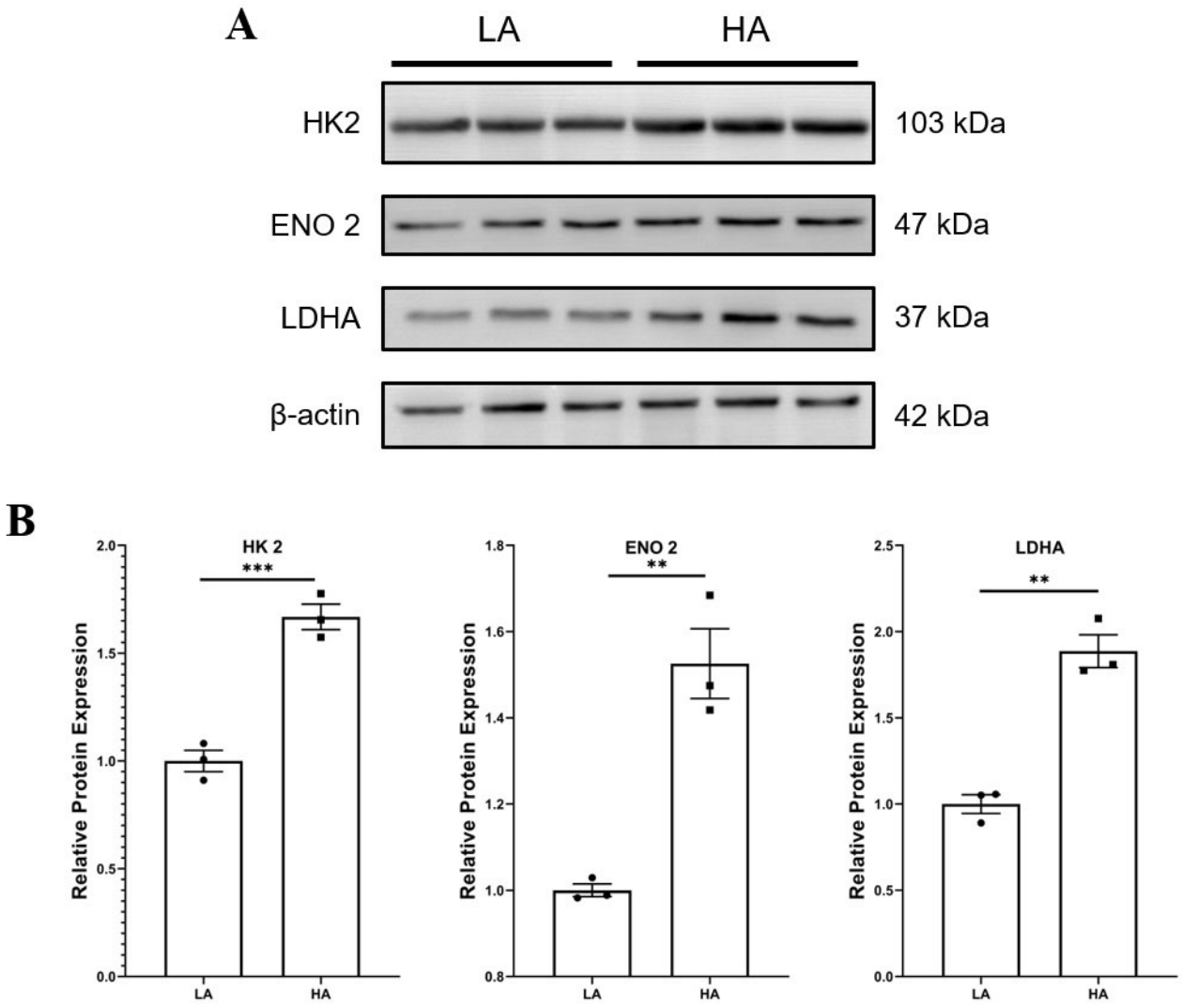

Fig. 8. Western blot validation of HK2, ENO2, and LDHA protein expression in sheep pituitaries. (A) Representative Western blot images of HK2, ENO2, and LDHA in the LA and HA groups, with β-actin used as the loading control. (B) Densitometric analysis of the relative protein expression levels of HK2, ENO2, and LDHA in the LA and HA groups. ** $p < 0.01$; *** $p < 0.001$.

each group. This design helped reduce variation related to sex, age, and reproductive status, although confirmation in larger and more diverse cohorts would further strengthen the findings. The HA and LA groups represented locally predominant breeds raised under their native regional conditions, so genetic background and environmental factors may have contributed to the observed expression patterns. In addition, pituitary morphology, circulating hormones, and other relevant endocrine and metabolic indicators were beyond the scope of the present study. The current results provide expression-level evidence for remodeling of selected glycolysis–lactate-related nodes, and future studies incorporating functional endocrine and metabolic assessments will help clarify their physiological significance.

Limitations

This study has several limitations. First, the sample size was limited to three animals per group. Although the use of adult non-pregnant ewes of similar age helped reduce variation related to sex, age, and reproductive status, the small-sample design may still limit the statistical power of the study. Second, the HA and LA groups were derived from different breeds and different regions, so genetic background and environmental factors may have contributed to the observed pituitary expression patterns. Therefore, the present findings should be interpreted cautiously and should not be attributed exclusively to hypoxia itself. Third, pituitary morphology, circulating hormones, and other relevant endocrine and metabolic indicators were beyond the scope of the present study. Therefore, the current results mainly provide expression-level evidence for changes in se-

lected glycolysis–lactate metabolism-related nodes. Future studies combining larger sample sizes, metabolic measurements, and functional experiments will be needed to further clarify the physiological significance of these findings.

5. Conclusions

Integrated transcriptomic–proteomic analysis and targeted validation identified concordant upregulation of HK2, ENO2, and LDHA in the pituitary samples of high-altitude sheep. These findings indicate remodeling of selected expression nodes associated with glycolysis and pyruvate-to-lactate conversion. Their effects on metabolic flux, energy production, and pituitary endocrine function require direct functional validation.

Availability of Data and Materials

The RNA-seq data generated in this study have been deposited in the Genome Sequence Archive under accession number CRA036804. The proteomic data have been deposited in iProX under accession number IPX0015095000. The datasets utilized and analyzed in the current study are available from the corresponding author upon reasonable request.

Author Contributions

FM participated in experimental design, sample processing, data analysis, experimental validation, and manuscript drafting. XL was responsible for study conception, experimental design, funding acquisition, and manuscript revision. XD and HW participated in sample collection, coordination of experimental materials, and interpretation of the data. All authors contributed to editorial changes in the manuscript. All authors read and approved the final manuscript. All authors have participated sufficiently in the work and agreed to be accountable for all aspects of the work.

Ethics Approval and Consent to Participate

The animal experimental protocol was approved by the Animal Ethics Committee of Gansu Agricultural University (approval No. GSAU-Eth-LST-2023-004). All animal sampling and experimental procedures were conducted in accordance with the ethical requirements of the Animal Ethics Committee of Gansu Agricultural University and the Chinese national standard GB/T 35892-2018, Laboratory animal—Guideline for ethical review of animal welfare, and followed the principles of the 3Rs (Replacement, Reduction, and Refinement). The study was reported in accordance with the ARRIVE guidelines for animal research.

Acknowledgment

The graphical abstract was created using Adobe Illustrator (Adobe Inc., San Jose, CA, USA).

Funding

This work was supported by the National Natural Science Foundation of China (31760305), Screening and Identification of the Core Population of Qilian White Tibetan Sheep (GSAU-JSFW-2023-79), and Detection and Analysis of Blood Physiological and Biochemical Indicators in Qilian White Tibetan Sheep (GSAU-JSFW-2025-69).

Conflicts of Interest

The authors declare no conflicts of interest.

Declaration of AI and AI-Assisted Technologies in the Writing Process

ChatGPT (GPT-5.6, OpenAI) was used during manuscript drafting and language polishing. The authors reviewed, revised, and approved the entire manuscript and take full responsibility for its accuracy, completeness, and academic integrity.

Supplementary Material

Supplementary material associated with this article can be found, in the online version, at https://doi.org/10.31083/FBL54255.

References

[1] Zhang C, Wu Y, Wang S, Li M, Tian H, Li S. Adaptive Regulation of Glucose Metabolism and Diseases in High-Altitude Areas. Sichuan Da Xue Xue Bao. Yi Xue Ban = Journal of Sichuan University. Medical Science Edition. 2024; 55: 1460–1468. https://doi.org/10.12182/20241160604 (In Chinese)

[2] Yan Z, Yang J, Wei WT, Zhou ML, Mo DX, Wan X, et al. A time-resolved multi-omics atlas of transcriptional regulation in response to high-altitude hypoxia across whole-body tissues. Nature Communications. 2024; 15: 3970. https://doi.org/10.1038/s41467-024-48261-w

[3] Wang GL, Jiang BH, Rue EA, Semenza GL. Hypoxia-inducible factor 1 is a basic-helix-loop-helix-PAS heterodimer regulated by cellular O2 tension. Proceedings of the National Academy of Sciences of the United States of America. 1995; 92: 5510–5514. https://doi.org/10.1073/pnas.92.12.5510

[4] Song Y, Yuan C, Guo T, Chen B, Wang F, Lu Z, et al. Genome-wide selection signal analysis reveals the adaptability of Tibetan sheep to high altitudes. Frontiers in Veterinary Science. 2025; 12: 1632017. https://doi.org/10.3389/fvets.2025.1632017

[5] Lin J, Fan L, Han Y, Guo J, Hao Z, Cao L, et al. The mTORC1/eIF4E/HIF-1α Pathway Mediates Glycolysis to Support Brain Hypoxia Resistance in the Gansu Zokor, *Eospalax cansus*. Frontiers in Physiology. 2021; 12: 626240. https://doi.org/10.3389/fphys.2021.626240

[6] Wen Y, Wang J, Liu X, Li S, Hu J, Luo Y. Regulating glycolysis and heat shock proteins in Gannan yaks (*Bos grunniens*) in response to hypoxia of the Qinghai-Tibet Plateau. Archives Animal Breeding. 2021; 64: 345–353. https://doi.org/10.5194/aab-64-345-2021

[7] He Z, Li S, Zhao F, Sun H, Hu J, Wang J, et al. LncRNA and Protein Expression Profiles Reveal Heart Adaptation to High-Altitude Hypoxia in Tibetan Sheep. International Journal of Molecular Sciences. 2023; 25: 385. https://doi.org/10.3390/ijms25010385

[8] Viña JR, Page RB, Davis DW, Hawkins RA. Aerobic glycoly-

sis by the pituitary gland in vivo. Journal of Neurochemistry. 1984; 42: 1479–1482. https://doi.org/10.1111/j.1471-4159.1984.tb02814.x

[9] Wang TY, Xia FY, Gong JW, Xu XK, Lv MC, Chatoo M, et al. CRHR1 mediates the transcriptional expression of pituitary hormones and their receptors under hypoxia. Frontiers in Endocrinology. 2022; 13: 893238. https://doi.org/10.3389/fendo.2022.893238

[10] Chen S, Zhou Y, Chen Y, Gu J. fastp: an ultra-fast all-in-one FASTQ preprocessor. Bioinformatics (Oxford, England). 2018; 34: i884–i890. https://doi.org/10.1093/bioinformatics/bty560

[11] Langmead B, Salzberg SL. Fast gapped-read alignment with Bowtie 2. Nature Methods. 2012; 9: 357–359. https://doi.org/10.1038/nmeth.1923

[12] Kim D, Paggi JM, Park C, Bennett C, Salzberg SL. Graph-based genome alignment and genotyping with HISAT2 and HISAT-genotype. Nature Biotechnology. 2019; 37: 907–915. https://doi.org/10.1038/s41587-019-0201-4

[13] Li B, Dewey CN. RSEM: accurate transcript quantification from RNA-Seq data with or without a reference genome. BMC Bioinformatics. 2011; 12: 323. https://doi.org/10.1186/1471-2105-12-323

[14] Love MI, Huber W, Anders S. Moderated estimation of fold change and dispersion for RNA-seq data with DESeq2. Genome Biology. 2014; 15: 550. https://doi.org/10.1186/s13059-014-0550-8

[15] Gillet LC, Navarro P, Tate S, Röst H, Selevsek N, Reiter L, et al. Targeted data extraction of the MS/MS spectra generated by data-independent acquisition: a new concept for consistent and accurate proteome analysis. Molecular & Cellular Proteomics: MCP. 2012; 11: O111.016717. https://doi.org/10.1074/mcp.O111.016717

[16] Escher C, Reiter L, MacLean B, Ossola R, Herzog F, Chilton J, et al. Using iRT, a normalized retention time for more targeted measurement of peptides. Proteomics. 2012; 12: 1111–1121. https://doi.org/10.1002/pmic.201100463

[17] Barkovits K, Pacharra S, Pfeiffer K, Steinbach S, Eisenacher M, Marcus K, et al. Reproducibility, Specificity and Accuracy of Relative Quantification Using Spectral Library-based Data-independent Acquisition. Molecular & Cellular Proteomics: MCP. 2020; 19: 181–197. https://doi.org/10.1074/mcp.RA119.001714

[18] Ashburner M, Ball CA, Blake JA, Botstein D, Butler H, Cherry JM, et al. Gene ontology: tool for the unification of biology. The Gene Ontology Consortium. Nature Genetics. 2000; 25: 25–29. https://doi.org/10.1038/75556

[19] Okuda S, Yamada T, Hamajima M, Itoh M, Katayama T, Bork P, et al. KEGG Atlas mapping for global analysis of metabolic pathways. Nucleic Acids Research. 2008; 36: W423–W426. https://doi.org/10.1093/nar/gkn282

[20] Subramanian A, Tamayo P, Mootha VK, Mukherjee S, Ebert BL, Gillette MA, et al. Gene set enrichment analysis: a knowledge-based approach for interpreting genome-wide expression profiles. Proceedings of the National Academy of Sciences of the United States of America. 2005; 102: 15545–15550. https://doi.org/10.1073/pnas.0506580102

[21] Schneider CA, Rasband WS, Eliceiri KW. NIH Image to ImageJ: 25 years of image analysis. Nature Methods. 2012; 9: 671–675. https://doi.org/10.1038/nmeth.2089

[22] Semenza GL. Regulation of metabolism by hypoxia-inducible factor 1. Cold Spring Harbor Symposia on Quantitative Biology. 2011; 76: 347–353. https://doi.org/10.1101/sqb.2011.76.010678

[23] Kierans SJ, Taylor CT. Regulation of glycolysis by the hypoxia-inducible factor (HIF): implications for cellular physiology. The Journal of Physiology. 2021; 599: 23–37. https://doi.org/10.1113/JP280572

[24] Pang Y, Hu S, Wen B, Wu D, Song F, Yin J, et al. Expression Regulation of Gluconeogenesis Related Genes in Ovine Skeletal Muscle Cells. Frontiers in Bioscience (Landmark edition). 2024; 29: 237. https://doi.org/10.31083/j.fbl2906237

[25] Brooks GA. The Science and Translation of Lactate Shuttle Theory. Cell Metabolism. 2018; 27: 757–785. https://doi.org/10.1016/j.cmet.2018.03.008

[26] Hui S, Ghergurovich JM, Morscher RJ, Jang C, Teng X, Lu W, et al. Glucose feeds the TCA cycle via circulating lactate. Nature. 2017; 551: 115–118. https://doi.org/10.1038/nature24057

[27] Rabinowitz JD, Enerbäck S. Lactate: the ugly duckling of energy metabolism. Nature Metabolism. 2020; 2: 566–571. https://doi.org/10.1038/s42255-020-0243-4

[28] Kim JW, Tchernyshyov I, Semenza GL, Dang CV. HIF-1-mediated expression of pyruvate dehydrogenase kinase: a metabolic switch required for cellular adaptation to hypoxia. Cell Metabolism. 2006; 3: 177–185. https://doi.org/10.1016/j.cmet.2006.02.002

[29] Papandreou I, Cairns RA, Fontana L, Lim AL, Denko NC. HIF-1 mediates adaptation to hypoxia by actively downregulating mitochondrial oxygen consumption. Cell Metabolism. 2006; 3: 187–197. https://doi.org/10.1016/j.cmet.2006.01.012

[30] Storz JF, Scott GR, Cheviron ZA. Phenotypic plasticity and genetic adaptation to high-altitude hypoxia in vertebrates. The Journal of Experimental Biology. 2010; 213: 4125–4136. https://doi.org/10.1242/jeb.048181

[31] Bigham AW, Lee FS. Human high-altitude adaptation: forward genetics meets the HIF pathway. Genes & Development. 2014; 28: 2189–2204. https://doi.org/10.1101/gad.250167.114

[32] Cheviron ZA, Brumfield RT. Genomic insights into adaptation to high-altitude environments. Heredity. 2012; 108: 354–361. https://doi.org/10.1038/hdy.2011.85